Supporting Information

Facile approach to deposit high performance electrocatalyst high entropy oxide coatings using a novel plasma spray route for efficient water splitting in alkaline medium

Amarnath Pasupathi,[1] Praveen Kandasamy,[2,3] Ranjith Kumar Dharman,[4] Sivakumar Govindarajan,[2] Tae Hwan Oh,[4] Min Wook Lee,[3] and Yugeswaran Subramaniam [1*]

[1]Applied Thermal Plasma Laboratory, Department of Physics, Pondicherry University, Puducherry 605014, India.

[2]Centre for Engineered Coatings, International Advanced Research Centre for Powder Metallurgy and New Materials, Balapur, Hyderabad 500 005, Telangana, India.

[3]Institute of Advanced Composite Materials, Korea Institute of Science and Technology, Chudong-ro, Bongdong-eup, Jeonbuk 55324, Republic of Korea.

[4]School of Chemical Engineering, Yeungnam University, Gyeongsan 38541, South Korea.

**Corresponding author's email: yugeswaran@pondiuni.ac.in*

This file contains 13 pages in which the information on CV, Cdl, comparison tables, Post studies, references are given respectively.

Number of Figure: 6 (S1-S6)

Number of Table: 2 (S1-S2)

Electrochemical characterization

All the potential data were converted into an RHE scale according to the following equation:

$$E_{RHE}= E_{ref} + 0.098 + 0.059pH \ldots\ldots\ldots\ldots\ldots\ldots \text{equation 1}$$

Overpotential

The overpotential values of all the catalysts were calculated at a benchmarking current density of 10 mA cm^{-2} by employing the following relation:

$$\eta_{10}(OER)=(E_{obs}-1.23) \text{ V versus RHE} \ldots\ldots\ldots\ldots\ldots\ldots \text{equation 2}$$

$$\eta_{10}(HER)=(0-E_{obs}) \text{ V versus RHE} \ldots\ldots\ldots\ldots\ldots\ldots \text{equation 3}$$

The Tafel Slope

The Tafel slope was calculated by fitting the overpotential versus log (j) using the Tafel equation as given below:

$$\eta=b \times \log (j/j_o) \ldots\ldots\ldots\ldots\ldots\ldots \text{equation 4}$$

where "b" signifies the Tafel slope value, "j" implies the current density value, and "j_0" is the exchange current density. Electrochemical impedance spectroscopy (EIS) measurements were done on the frequency ranges from 100 Hz to 0.1 Hz with an amplitude of 5 mV in 1 M KOH solution. The long-term durability study was performed using chronopotentiometry measurement.

Electrochemical Active Surface Area (ECSA)

The electrochemical active surface areas (ECSA) were measured by determining the electrochemical C_{dl} using the following equations:

$$i_c= \nu \times C_{dl} \ldots\ldots\ldots\ldots\ldots\ldots \text{equation 5}$$

$$ECSA= C_{dl}/C_s \ldots\ldots\ldots\ldots\ldots\ldots \text{equation 6}$$

where "i_c" indicates the double-layer charging current resulting from scan-rates (ν) dependent CVs at non-faradic potential, and "C_s" denotes a specific capacitance value of 0.040 mF cm^{-2} for flat electrodes.

Turnover Frequency (TOF)

The amount of oxygen/hydrogen that is evolved per unit of time is known as the TOF. The TOF of the catalyst can be determined by the below expression,

$$TOF = \frac{j \times N_A}{n \times F \times \tau} \qquad \text{..................equation 7}$$

where, j = current density, N_A= Avogadro number, F = Faraday constant (96 485 C mol^{-1}), n = Number of electrons (For OER, n = 4 and HER, n = 2), Γ = Surface concentration.

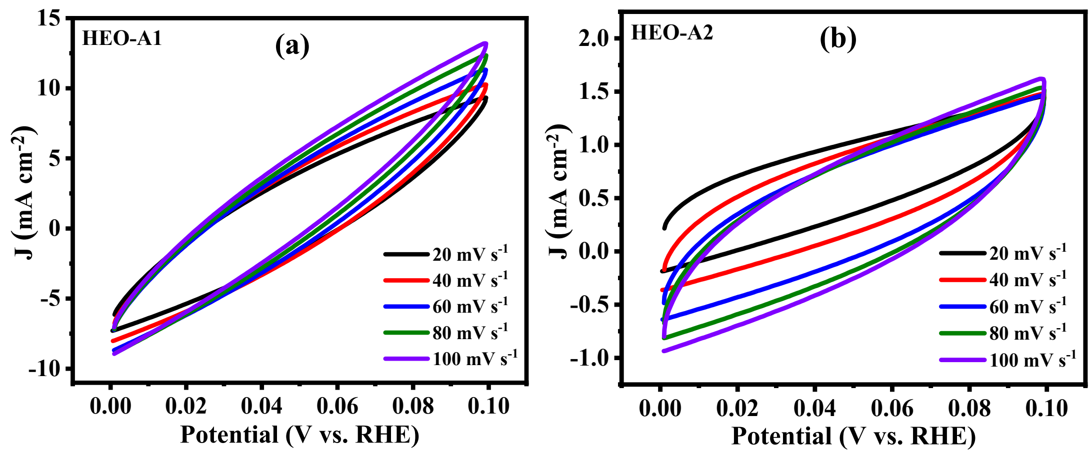

Figure S1. (a and b) CVs at different scan rates in the non-faradaic area to determine the C_{dl} values of HEO-A1 and HEO-A2, respectively.

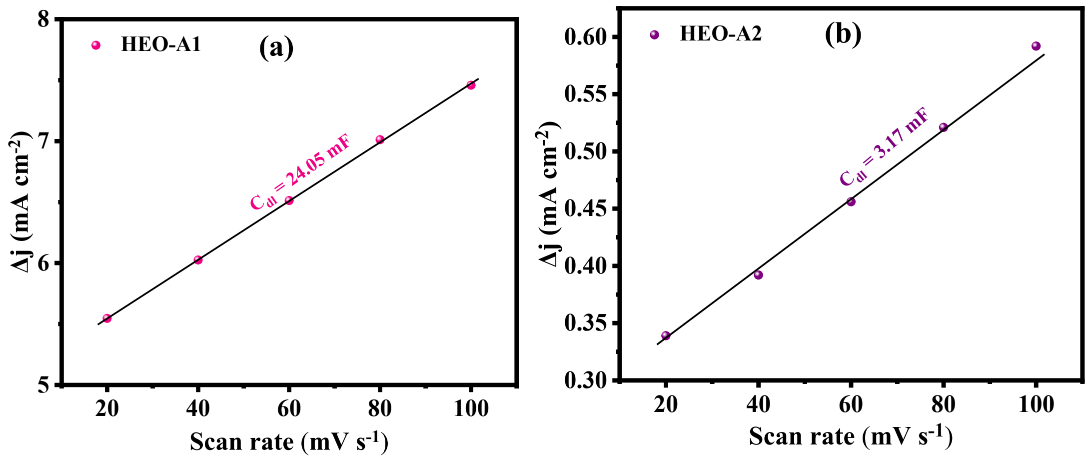

Figure S2. (a and b) Calculated C_{dl} values of HEO-A1 and HEO-A2.

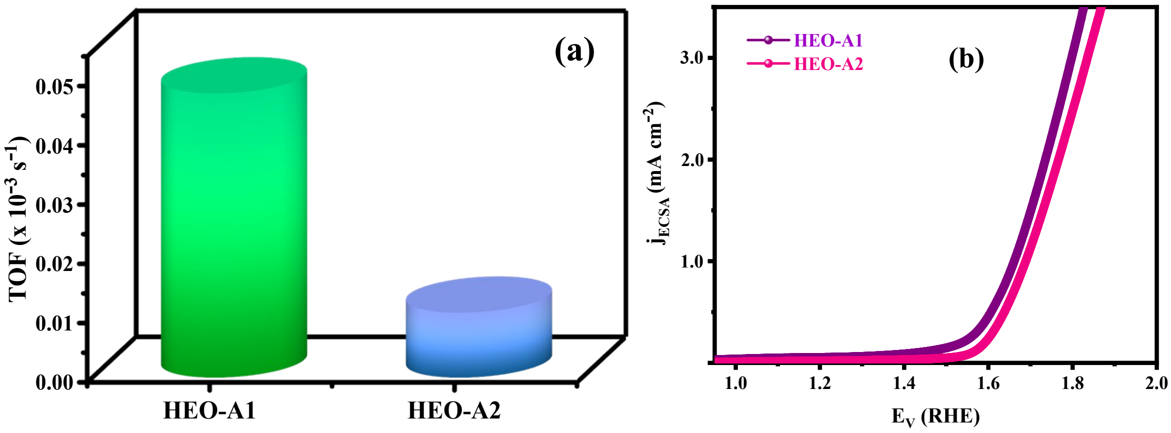

Figure. S4 (a) TOF and (b) ESCA normalized LSV curve of HEO-A1, and HEO-A2.

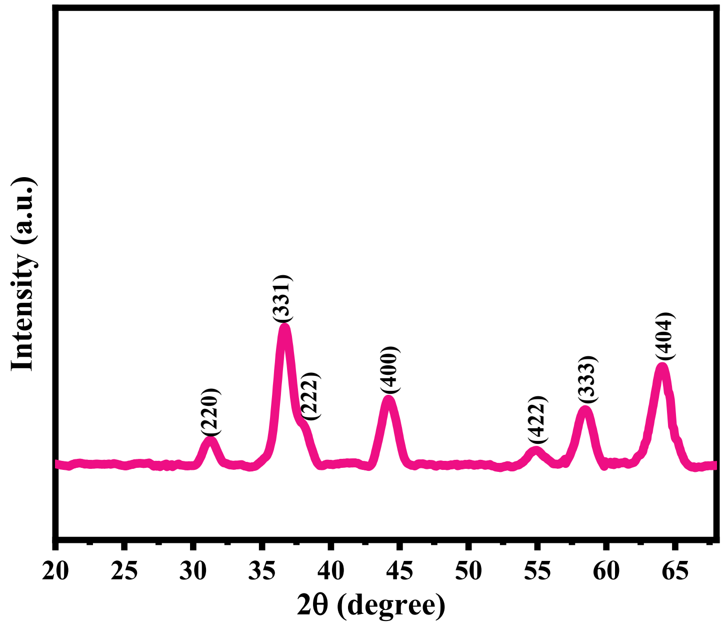

Figure. S4 XRD pattern of HEO-A1 coating after stability test.

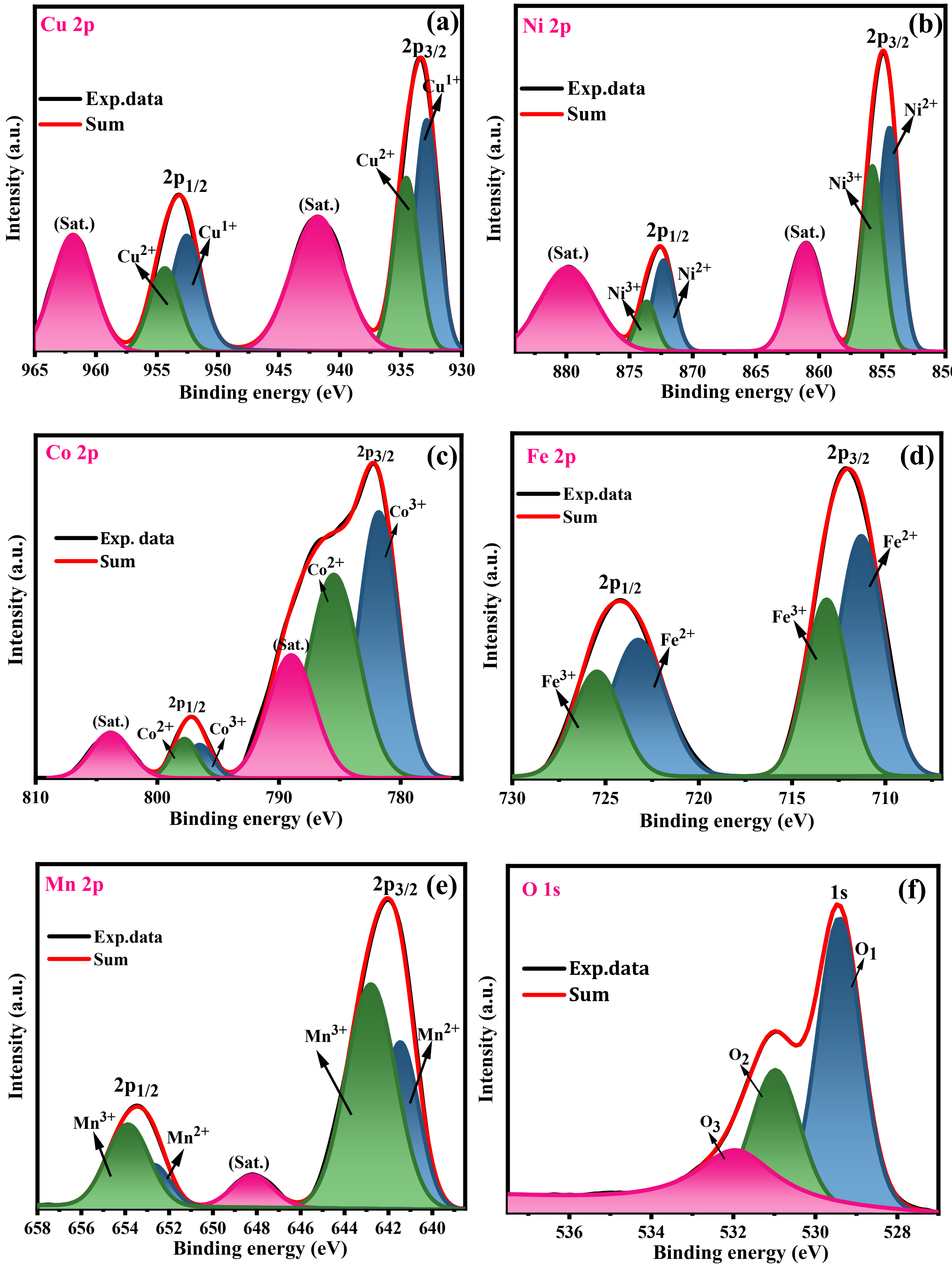

Figure. S5 XPS spectra of HEO A1 coating after electrochemical performance analysis: (a) Co 2p, (b) Fe 2p, (c) Mn 2p, (d) Ni 2p, (e) Cu 2p, and (f) O 1s.

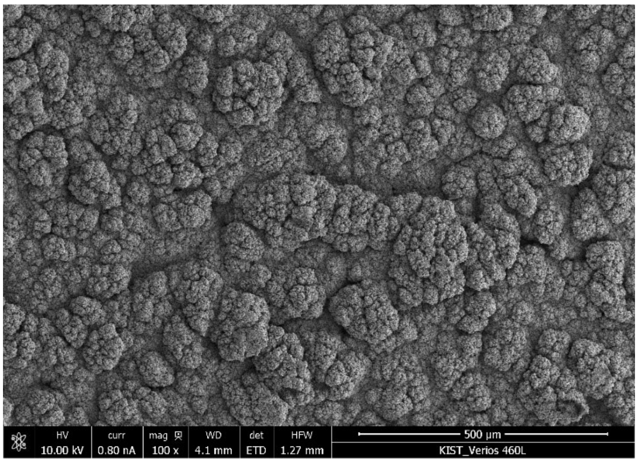

Figure. S6 Surface morphology of HEO-A1 coating after electrochemical performance analysis.

S. No	Electrocatalyst	Overpotential (mV)	Tafel slope (mV/dec)	Current density	Reference

				(mA cm^{-2})	
1	(Fe, Co, Ni, Mn, B)O_x	266	64.5	10	[1]
2	(Ir, Ru, Cr, Fe, Co, Ni)O_x	190	51.1	10	[2]
3	(Fe, Ni, Co, Cr, Mn)$_2O_3$	174	68	10	[3]
4	La(Cr, Mn, Fe, Co, Ni)O_3	325	51.2	10	[4]
5	(Li, Fe, Co, Ni, Cu, Zn)O	347	79.4	10	[5]
6	(Co, Ni, Mn, Zn, Fe)$_3O_{3.2}$	336	47.5	10	[6]
7	(Mg, Fe, Co, Ni, Cu)$_3O_4$	300	40	10	[7]
8	(Fe, Co, Ni, Cr, Mn)$_3O_4$	288	60	10	[8]
9	(Mn, Fe, Co, Ni, Zn)$_3O_4$	330	36.7	10	[9]
10	(Mn, Fe, Ni, Mg, Cr)$_3O_4$	293	46.5	10	[10]
11	(Co, Fe, Ni, Cr, Mn)$_3O_4$	309	48.5	10	[11]
12	(Co, Cr, Fe, Mn, Ni)$_3O_4$	220	100	10	[12]
13	(Cr, Mn, Fe, Ni, Zn)$_3O_4$	295	53.7	10	[13]
14	(Co, Ni, Zn, Fe, Mn)$_3O_4$	265	83.7	10	[14]
15	(Ni, Fe, Mn, Cu, Zn)$_3O_4$	308	54	50	[15]
16	(Ni, Co, Cr, Mn, V)$_3O_4$	247	54	50	[16]
17	(Ni, Co, Cr, Mn, Mo)$_3O_4$	246	38	50	[17]
18	(Ni, Fe, Co, Cu, Mn)$_3O_4$	220	46	10	This work

Table S1. Comparison of high entropy oxides (HEOs) based electrocatalyst for OER application in 1 M KOH electrolyte solution.

S. No	**Electrocatalyst**	**Overpotential (mV)**	**Tafel slope (mV/dec)**	**Current density (mA cm^{-2})**	**Reference**
1	(Fe, Ni, Co, Cr, Mn)$_2O_3$	60	80	10	[3]

2	(Li, Fe, Co, Ni, Cu, Zn)O	207	79.4	10	[5]
3	(Fe, Ni, Co, Mn, V)$_3$O$_4$	81	88	10	[18]
4	(Fe, Co, Ni, Cu, Zn)$_3$O$_4$	67	77	10	[19]
5	(Ni, Co, Cr, Mn, V)$_3$O$_4$	217	92	50	[16]
6	(Ni, Co, Cr, Mn, Mo)$_3$O$_4$	197	93	50	[17]
7	(Ni, Fe, Co, Cu, Mn)$_3$O$_4$	129	43	10	This work

Table S2. Comparison of high entropy oxides (HEOs) based electrocatalyst for HER application in 1 M KOH electrolyte solution.

References

1 S. Jiang, K. Tian, X. Li, C. Q. Duan, D. Wang, Z. Wang, H. Sun, R. Zheng and Y. Liu, *J. Colloid Interface Sci.*, 2022, 606, 635–644.

2 W. Rong, Y. Chen, R. Dang, K. Huang, J. Xia, B. Zhang, J. Liu, H. Meng, Q. Cao and

J. Wu, *J. Alloys Compd.*, 2024, **971**, 172786.

3 S. Liao, T. Huang, W. Wu, T. Yang, Q. Hou, S. Sang, K. Liu, Y. Yang and H. Liu, *Chem. Eng. J.*, 2023, **471**, 144506.

4 T. X. Nguyen, Y. C. Liao, C. C. Lin, Y. H. Su and J. M. Ting, *Adv. Funct. Mater.*, 2021, **31**, 1–10.

5 Y. Gu, A. Bao, X. Wang, Y. Chen, L. Dong, X. Liu, H. Pan, Y. Li and X. Qi, *Nanoscale*, 2022, **14**, 515–524.

6 Y. Zhang, W. Dai, P. Zhang, T. Lu and Y. Pan, *J. Alloys Compd.*, 2021, **868**, 159064.

7 T. X. Nguyen, Z. T. Huang and J. M. Ting, *Appl. Surf. Sci.*, 2021, **570**, 151160.

8 C. Duan, X. Li, D. Wang, Z. Wang, H. Sun, R. Zheng and Y. Liu, *Sustain. Energy Fuels*, 2022, **6**, 1479–1488.

9 Xiaolin, K. Iwase and Honma, *J. Mater. Chem. A*, 2022, **5**, 9292–9296.

10 D. Stenzel, B. Zhou, C. Okafor, M. V. Kante, L. Lin, G. Melinte, T. Bergfeldt, M. Botros, H. Hahn, B. Breitung and S. Schweidler, *Front. Energy Res.*, 2022, **10**, 1–11.

11 J. Baek, D. Hossain, P. Mukherjee, J. Lee, K. Winther, Y. Jiang, W. Chueh, M. Bajdich and X. Zheng, 2022, 1–22.

12 B. Talluri, K. Yoo and J. Kim, *J. Environ. Chem. Eng.*, 2022, **10**, 106932.

13 X. Yang, S. Liping, L. Qiang, H. Lihua and Z. Hui, *J. Mater. Chem. A*, 2022, **10**, 17633–17641.

14 M. Li, M. Song, W. Ni, Z. Xiao, Y. Li, J. Jia, S. Wang and Y. Wang, *Chinese Chem. Lett.*, 2023, **34**, 107571.

15 P. Amarnath, R. Madhu, K. Praveen, S. Govindarajan, S. Kundu and Y. Subramaniam, *ACS Appl. Energy Mater.*, 2023, **6**, 5899–5911.

16 A. Pasupathi, R. Madhu, S. Kundu and Y. Subramaniam, *Electrochim. Acta*, 2024, **497**, 144621.

17 A. Pasupathi, R. Madhu, S. Kundu and Y. Subramaniam, *J. Power Sources*, 2025, **630**, 236144.

18 S. Ding, Y. Sun, F. Lou, L. Yu, B. Xia, J. Duan, Y. Zhang and S. Chen, *J. Power Sources*, 2022, 520.

19 J. Du, X. Zhang, F. He and Y. Xie, *Electrochim. Acta*, 2023, **461**, 142599.